

# Ultrahigh-pressure induced decomposition of silicon disulfide into silicon-sulfur compounds with high coordination numbers

**HPSTAR**  
**763-2019**

 Yuanzheng Chen,<sup>1,\*</sup> Xiaolei Feng,<sup>2,3,4,†</sup> Jiao Chen,<sup>1</sup> Xinyong Cai,<sup>1</sup> Bai Sun,<sup>1,5</sup> Hongyan Wang,<sup>1</sup> Huarong Du,<sup>1</sup> Simon A. T. Redfern,<sup>3,4</sup> Yu Xie,<sup>6,‡</sup> and Hanyu Liu<sup>6,§</sup>
<sup>1</sup>*School of Physical Science and Technology, Key Laboratory of Advanced Technologies of Materials, Southwest Jiaotong University, Chengdu 610031, China*
<sup>2</sup>*The Institute for Disaster Management and Reconstruction, Sichuan University, Chengdu, 610207, China*
<sup>3</sup>*Center for High Pressure Science and Technology Advanced Research (HPSTAR), Beijing 100094, China*
<sup>4</sup>*Department of Earth Sciences, University of Cambridge, Cambridge, CB2 3EQ, United Kingdom*
<sup>5</sup>*Department of Mechanics and Mechatronics Engineering, Centre for Advanced Materials Joining, Waterloo Institute of Nanotechnology, and Department of Physics and Astronomy, University of Waterloo, Waterloo, Ontario, Canada N2L 3G1*
<sup>6</sup>*Innovation Center for Computational Physics Methods and Software & State Key Lab of Superhard Materials, College of Physics, Jilin University, Changchun 130012, China*


(Received 31 January 2019; revised manuscript received 24 April 2019; published 15 May 2019)

Silicon disulfide, SiS<sub>2</sub>, is thought to occur in interstellar dust and is of fundamental interest more generally among the silicon chalcogenides as a comparator to SiO<sub>2</sub>, an important component of terrestrial planets. However, the high-pressure behaviors of silicon sulfides are unclear. Here, using an efficient structure search method, we systematically explore the structural evolution of different Si-S stoichiometries up to 250 GPa. SiS<sub>2</sub> is found to be stable below 155 GPa, above which it decomposes into two compounds, SiS and SiS<sub>3</sub>. SiS adopts a high-symmetry cubic structure consisting of eightfold-coordinated silicon in face-sharing SiS<sub>8</sub> polyhedra, while SiS<sub>3</sub> crystallizes in a rhombohedral structure containing ninefold-coordinated SiS<sub>9</sub> polyhedra. Analyses suggest that the Si eightfold-coordination environment could be a common feature for group IV–VI compounds under high pressure. Our findings provide insights on the nature of Si-S compounds under ultrahigh pressure.

 DOI: [10.1103/PhysRevB.99.184106](https://doi.org/10.1103/PhysRevB.99.184106)

## I. INTRODUCTION

Being one of the most abundant elements in the Solar System, silicon is also rich in Earth and other terrestrial planets such as Mars and Venus, where it typically exists in crystalline compounds [1,2]. Studies of silicon chalcogenides are dominated by those focused on silicon oxide such as quartz that forms the second most abundant mineral in Earth's crust. In contrast, silicon sulfides, which are suggested to form an important component of interstellar dust [3,4], are not yet well understood. Understanding the behavior of silicon sulfide phases under high pressure (HP) is therefore important and may shed light on the structural properties of silicon chalcogenides, more specifically the silicates, as these phases act as analogs of other HP compounds that might be formed in the important family of group IV–VI compounds (e.g., Si-O, Ge-O) [5–13].

The coordination number of silicon is of such great importance that the layering of the bulk silicate Earth is driven by density changes controlled by increasing silicon coordination by oxygen as silicates respond to increased pressure in Earth's interior. This is evidenced by the fact that bridgmanite,

MgSiO<sub>3</sub> perovskite, with silicon 6-coordinated by oxygen, is the major phase in the lower mantle [14,15], while ringwoodite, spinel Mg<sub>2</sub>SiO<sub>4</sub> phase, with 4-coordinated silicon, is stable at shallower depths [16]. In silicate glasses there is evidence for the existence of even higher coordination number (CN) at sufficiently higher pressures: Energy-dispersive x-ray diffraction measurements on SiO<sub>2</sub> glass up to 172 GPa revealed the presence of silicon coordinated by more than 6 oxygens, with CN being 6 to 6.8 [17]. In addition, germanium, in compressed GeO<sub>2</sub> glass, was found to have CN larger than 6, reaching as high as 7.4 [18]. Even larger CNs (larger than 8) of silicon and germanium have also been proposed in the cotunnite-type (CN = 9), Fe<sub>2</sub>P-type (CN = 9), and *I4/mmm* (CN = 10) structures of SiO<sub>2</sub> (GeO<sub>2</sub>) at ultrahigh pressures theoretically [19–21].

Silicon disulfide, SiS<sub>2</sub>, being isoelectronic with SiO<sub>2</sub> and GeO<sub>2</sub>, is a further key representative phase of AB<sub>2</sub>-type compounds in the IV–VI group compounds, and may yield insights into the general behavior of silicon at high pressure. At ambient pressure, Normal Pressure (NP)-SiS<sub>2</sub>, with a structure that has space-group symmetry *Ibam*, consists of distorted edge-sharing SiS<sub>4</sub> tetrahedra with fourfold-coordinated silicon, first characterized in 1935 by Zintl *et al.* [22]. Upon increasing pressure to 4 GPa, the NP-SiS<sub>2</sub> phase subsequently transforms into three HP phases denoted HP1-SiS<sub>2</sub> (2.8 GPa), HP2-SiS<sub>2</sub> (3.5 GPa), and HP3-SiS<sub>2</sub> (~4 GPa) [23–25]. These HP phases can be closely related to the NP-SiS<sub>2</sub> phase as they all contain fourfold-coordination silicon. Very recently, a HP *P-3m1*

\*cyz@calypso.org.cn

†xf232@cam.ac.uk

‡xieyu@jlu.edu.cn

§hanyuliu@jlu.edu.cn

phase with Si sixfold coordination has been theoretically predicted to be stable above 4 GPa and remains so up to at least 100 GPa [26], which is similar to the HP behavior of silicates. Following this prediction, the HP  $P-3m1$  phase was synthesized between 7.5 and 9 GPa [27] and is characterized by 6-coordinated silicon [28]. However, a coordination number for silicon larger than 6 remains unachieved. This raises the question: Can silicon be coordinated by more than 6 sulfur atoms in  $\text{SiS}_2$  or more generally, in other Si-S compounds with different chemical stoichiometry?

To address these questions, we have carried out crystal-structure searches within the silicon-sulfur system, in combination with first-principles energetic calculations. Our results reveal a number of HP compounds with a range of fixed stoichiometries in the  $\text{Si}_x\text{S}_{1-x}$  ( $0 < x < 1$ ) system and demonstrate the existence of Si-S compounds with CN greater than 6. Our enthalpy calculations show that  $\text{SiS}_2$  is stable below 155 GPa (with Si CN  $\leq 6$ ), before it decomposes into compounds with a stoichiometry of  $\text{SiS}$  and  $\text{SiS}_3$ . In these  $\text{SiS}$  and  $\text{SiS}_3$  phases, the CN of Si (by S) can reach as high as 8 or 9.

## II. COMPUTATION DETAILS

Structure searches on  $\text{Si}_x\text{S}_{1-x}$  ( $x = 2/3, 1/2, 1/3, 1/4, 1/5$ ) system have been conducted at varied pressures, representing conditions from Earth's surface to its core (0, 50, 100, 150, 200, and 250 GPa) using structure-prediction methods with the same name code as CALYPSO [29,30]. Such an approach has previously been successfully employed to investigate structures of various compounds under HP [31,32]. A thorough survey of the literature, moreover, as well as online databases (e.g., ICSD and MaterialProject) [33,34] for the group IV–VI  $AB_2$  compounds, including  $\text{CO}_2$ ,  $\text{SiO}_2$ ,  $\text{CS}_2$ , and  $\text{GeO}_2$ , was also considered. Structure searches for each stoichiometry were performed with a unit cell containing up to four formula units. Several hundreds to a thousand structures were typically predicted, before the most stable candidates for each composition in the Si-S system at each pressure were identified. First-principles total-energy calculations were carried out using density-functional theory (DFT) as implemented in the VASP code [35]. In the framework of DFT, the structural optimizations were achieved using exchange-correlation functional treated with generalized gradient approximation (GGA) using the Perdew-Burke-Ernzerhof density functional [36]. The electron projector-augmented wave (PAW) method [37] was employed with PAW potentials, where  $2s^22p^2$  and  $2s^22p^4$  were treated as valence electrons for Si and S, respectively. An energy cutoff of 800 eV for the plane-wave expansion was adopted and appropriate Monkhorst-Pack  $k$  meshes [38] of uniform spacing of  $2\pi \times 0.03 \text{ \AA}^{-1}$  were chosen during *ab initio* electronic-structure calculations. Phonon-dispersion relations were calculated for all equilibrium structures using the direct supercell approach as implemented in the PHONOPY code [39].

## III. RESULTS AND DISCUSSION

The relative thermodynamic stabilities of  $\text{Si}_x\text{S}_{1-x}$  compounds that we identified as candidate equilibrium structures at 0 K can be assessed by convex hulls. Any structure which

has an enthalpy on the convex hull is considered to be thermodynamically stable and experimentally synthesizable with respect to a mixture of end members or other intermediates. As has been discussed previously [32], a phase whose formation enthalpy lies on the local minimum of the convex hull can likely be fabricated in the laboratory. If a tie line is drawn to connect  $\Delta H(\alpha)$  and  $\Delta H(\beta)$ , and  $\Delta H(\gamma)$  falls beneath it, mixtures of  $\alpha$  and  $\beta$  are expected to react to form compound  $\gamma$ . Otherwise, should  $\Delta H(\gamma)$  fall above the tie line, compound  $\gamma$  will decompose into a mixture of compounds  $\alpha$  and  $\beta$ . At a given pressure, a convex hull depicts the formation enthalpy per atom of the most stable phases for each stoichiometry, derived from the relation  $\Delta H = H(\text{Si}_x\text{S}_{1-x}) - xH(\text{Si}) - (1-x)H(\text{S})$ , where  $\Delta H$  is the enthalpy of formation per atom and  $H$  represents the calculated enthalpy of the candidate structure per stoichiometric unit for each compound. Here, the experimentally and theoretically known structures of the elemental silicon ( $Fd-3m$ ,  $P6_3/mmc$ , and  $Fm-3m$ ) [40] and sulfur ( $I4_1/acd$ ,  $bcm$ , and  $\beta\text{-Po}$ ) [41,42] were used to compute the elemental enthalpies of Si and S at the corresponding pressures.

Convex hulls at different pressures are given in Fig. 1, which summarizes the thermodynamic stability of the Si-S compounds that emerged out of our structure searches. At low pressure, as shown in Figs. 1(a)–1(c), the  $\text{SiS}_2$  compound has the most negative enthalpy of formation and falls on the convex hull between Si and S, indicating that  $\text{SiS}_2$  is stable in the pressure range of 0–100 GPa. This is consistent with the results from Plašienka *et al.* [26], who reported that  $\text{SiS}_2$  exists up to at least 100 GPa. Moreover, we successfully reproduced the known phases for the  $\text{SiS}_2$  compound, including the *Ibam*,  $P2_1/c$ ,  $I-4_2d$ , and  $P-3m1$  structures and confirmed the observed sequence of phase transitions, namely  $\text{NP}(\text{Ibam}) \rightarrow \text{HP1}(P2_1/c) \rightarrow \text{HP2}(P2_1/c) \rightarrow \text{HP3}(I-4_2d) \rightarrow P-3m1$  [Fig. 2(a)], as reported previously in both theoretical and experimental investigations [23–28]. This agreement validates the effectiveness of our computational scheme, in particular when applied to the Si-S system under HP.

As pressure increases,  $\text{SiS}_2$  becomes relatively less stable when  $\text{SiS}$  and  $\text{SiS}_3$  emerge in the convex hull at 150 GPa [Fig. 1(d)]. At 200 GPa [Fig. 1(e)], the results indicate that  $\text{SiS}_2$  is unstable and decomposes into a mixture of  $\text{SiS}$  and  $\text{SiS}_3$  via a reaction of  $2\text{SiS}_2 \rightarrow \text{SiS} + \text{SiS}_3$ . On further increase of pressure up to 250 GPa, the convex hull shows that  $\text{SiS}_3$  decomposes into  $\text{SiS}$  and S via another reaction of  $\text{SiS}_3 \rightarrow \text{SiS} + 2\text{S}$  [Fig. 1(f)], and  $\text{SiS}$  becomes the only stable compound between elemental S and Si.

To determine the detailed decomposition pressure, the formation enthalpies of the decomposition products ( $\text{SiS} + \text{SiS}_3$  and  $\text{SiS} + \text{S}$ ) relative to that of  $\text{SiS}_2$  have been calculated as a function of pressure and are shown in Fig. 2(c). It is clear that  $\text{SiS}_2$  starts to decompose at the pressure of 155 GPa.  $\text{SiS}_2$  would also decompose into a mixture of  $\text{SiS} + \text{S}$  around 166 GPa. Above 230 GPa,  $\text{SiS}_3$  decomposes into  $\text{SiS}$  and S. The stable pressure ranges of the equilibrium phases for  $\text{SiS}$ ,  $\text{SiS}_2$ , and  $\text{SiS}_3$  compounds at ultrahigh pressure (50–250 GPa) are depicted in Fig. 2(d). The energetically favorable crystalline phase of  $\text{SiS}_2$ , with space group of  $P-3m1$ , becomes stable up to 155 GPa.  $\text{SiS}$  adopts an equilibrium cubic

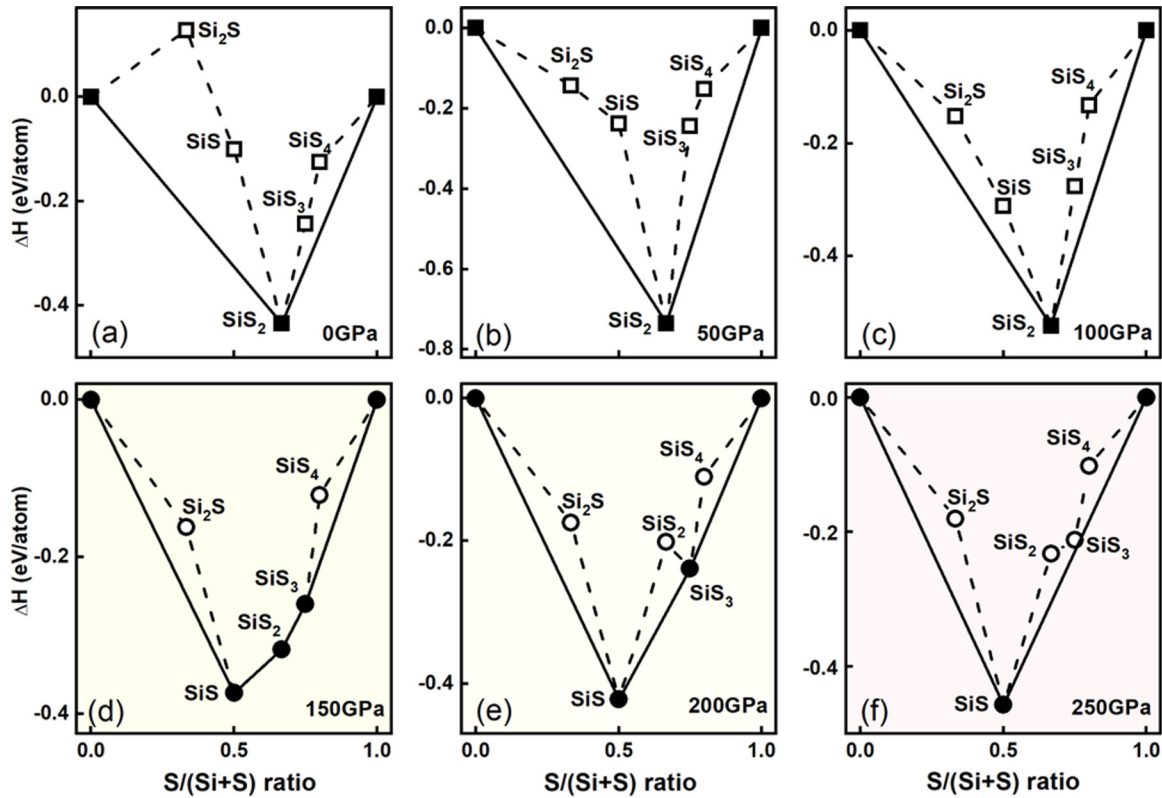


FIG. 1. Thermodynamic stability of Si-S compounds at both low and high pressures. The calculated enthalpy differences with respect to decomposition into Si and S from 0 to 250 GPa (a)–(f) are shown. Convex hulls are shown as solid lines, with stable compounds shown by solid symbols. Unstable compounds (open symbols) sit above convex hulls, with dashed lines indicating decomposition routes.

$Pm\bar{3}m$  structure at pressures of 155 to around 250 GPa, and  $\text{SiS}_3$  forms as trigonal  $R3m$  at 155 to 230 GPa. To verify our results, we also examined these predicted phase transitions and decomposition reactions using the local-density approximation functional. The pressure at which  $\text{SiS}_2$  decomposes to  $\text{SiS} + \text{SiS}_3$  was found to be  $\sim 145$  GPa, which agrees well with our GGA results.

To assess the dynamical stability of the predicted phases for the  $\text{SiS}$  and  $\text{SiS}_3$  compounds at each desired pressure, we calculated phonon-dispersion relations using the finite-displacement method [39]. Across the Brillouin zone we found no phonon branches with imaginary frequency values in any of the predicted structures ([Figs. 3(a) and 3(b)], indicating that they are dynamically stable. The  $\text{SiS}$  compound adopts a cubic structure in  $Pm\bar{3}m$  symmetry (space group 221,  $Z = 1$ ), as shown in Fig. 3(c), with Si and S occupying the  $1b$  (0.5, 0.5, 0.5) and  $1a$  (0, 0, 1) positions, respectively. In this structure, Si takes the sites on the top vertex of the hexahedron and each Si atom is coordinated with 8 S atoms and forms a regular hexahedron. Figure 3(d) shows the hexagonal  $\text{SiS}_3$  structure (space group  $R3m$ ,  $Z = 3$ ) with Si and S atoms occupying  $3a$  (0, 0, 0.396) and  $9b$  (0.523, 0.477, 0.262) positions, respectively. Here, each Si atom has 9 neighboring S atoms with Si-S distances range of 2.1–2.3 Å at 160 GPa, forming fairly regular tricapped trigonal prisms with Si ninefold-coordinated  $\text{SiS}_9$  polyhedra. The mean nearest-neighbor Si-S distances in the  $\text{SiS}$  and  $\text{SiS}_3$  phases are 2.23 and 2.27 Å at 160 GPa, respectively, which are

close to the sum of covalent radius of Si (1.11 Å) and S (1.02 Å). Interestingly, the Si-S distances in the HP  $\text{SiS}$  and  $\text{SiS}_3$  phases are even longer than that in the low-pressure  $\text{SiS}_2$  phase ( $P\bar{3}m1$ ) ( $\sim 2.17$  Å at 50 GPa), which may relate to the higher CN. Moreover, the S-S distances are found to be shorter in  $\text{SiS}$  and  $\text{SiS}_3$  than they are in  $\text{SiS}_2$ . In particular, the nearest-neighbor S-S distance decreases from 3.12 Å in the low-pressure  $\text{SiS}_2$  ( $P\bar{3}m1$ ) phase to 2.21 Å in the HP  $\text{SiS}_3$  ( $R3m$ ) structure, which is close to the sum (2.04 Å) of covalent radii of 2 S atoms. These results demonstrate that the increasing density (and hence stability) in the HP phases is achieved through the changes of polyhedral packing induced increasing of silicon CN and reduction of the nearest-neighbor S-S distances.

The discovery of eightfold Si in  $\text{SiS}$  at high pressure is quite fascinating since the CN of the group-IV atoms in the family of IV–VI  $AB_2$  compounds (IV = C, Si, Ge; VI = O, S) is generally four-, six-, nine-, and tenfold [43–46]. Significant efforts have been devoted to searching for solids containing 8-coordinated group-IV elements but with no success. It would be interesting to check whether  $\text{SiS}_2$  can form similar eightfold structures that may serve as the first prototype for IV–VI  $AB_2$  compounds, regardless of its thermal stability against decomposition. Further simulations showed [Fig. 2(b)] that  $\text{SiS}_2$  with the low-pressure  $P\bar{3}m1$  phase first transforms into a  $P4/mmm$  ( $>285$  GPa) phase, then to a  $Cmmm$  ( $>400$  GPa) phase upon compression (Fig. 4). It is found that the CN of silicon by sulfur is eightfold in both structures, the same as that of Si in the  $Pm\bar{3}m$

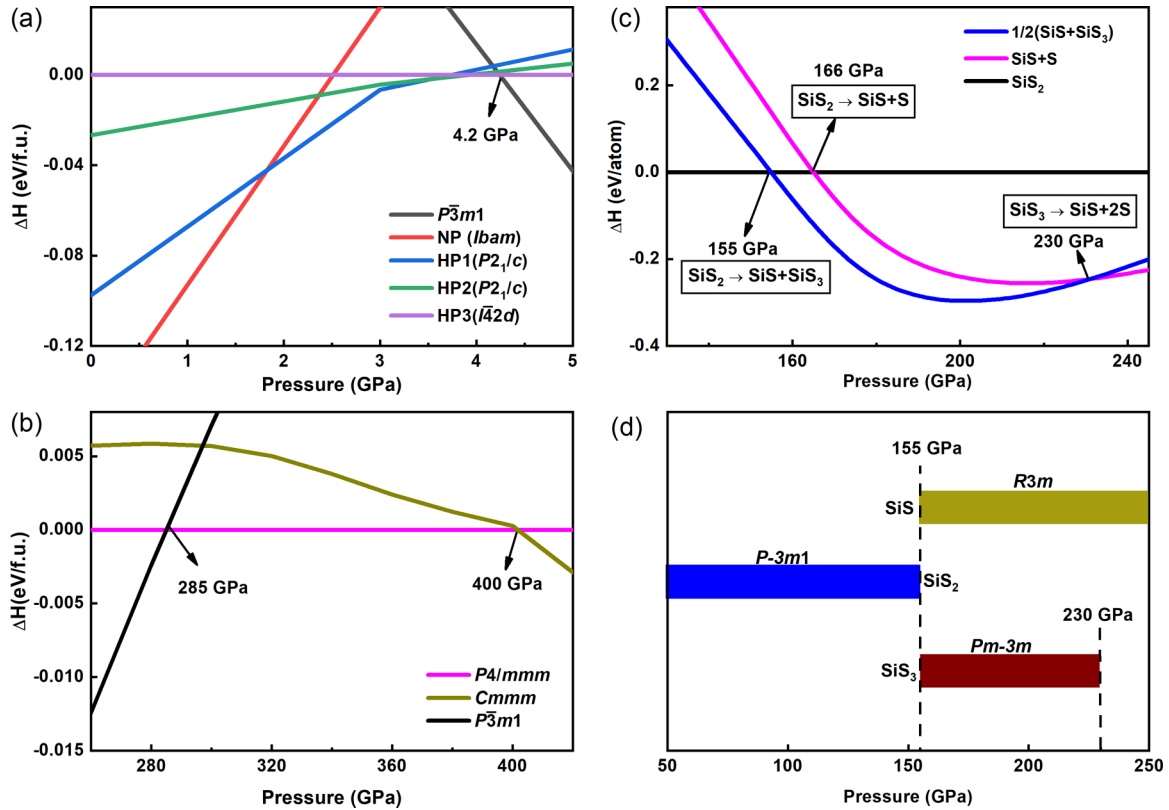


FIG. 2. Calculated enthalpy difference of HP phases for the  $\text{SiS}_2$  compound with respect to the  $P\bar{3}m1$  phase from 0 to 5 GPa (a) and from 260 to 420 GPa (b). (c) Calculated enthalpy differences ( $\Delta H$ ) of decomposition of  $\text{SiS}_2$  into  $\text{SiS} + \text{S}$  and  $\text{SiS} + \text{SiS}_3$  relative to  $\text{SiS}_2$  as functions of pressure (50–250 GPa). (d) Schematic representation of phase diagram for stable  $\text{SiS}$ ,  $\text{SiS}_2$ , and  $\text{SiS}_3$  compounds as a function of pressure.

phase of  $\text{SiS}$ . We also examined the stability of the ninefold cotunnite- and  $\text{Fe}_2\text{P}$ -type and tenfold  $I4/mmm$  structures [19–21] that have been observed in the HP phases of  $\text{SiO}_2$

and  $\text{GeO}_2$  for  $\text{SiS}_2$ . The results indicate that eightfold  $\text{SiS}_2$  is stable over a wide range of pressures and ninefold is only stable above 870 GPa.

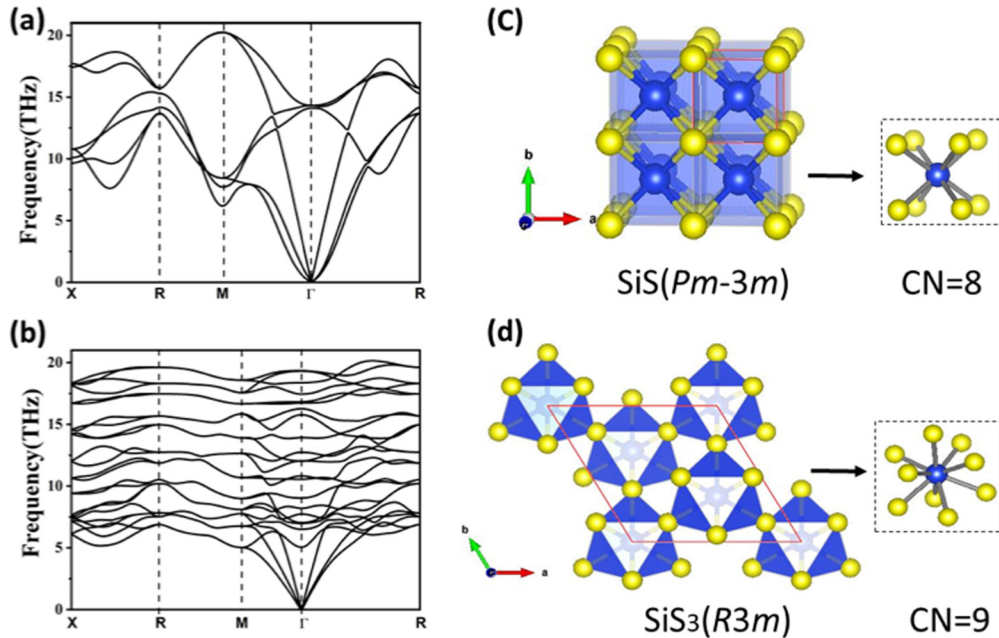


FIG. 3. Phonon-dispersion curves for the  $Pm\bar{3}m$  phase of  $\text{SiS}$  at 160 GPa (a) and the  $R3m$  of  $\text{SiS}_3$  at 200 GPa (b). Stable structures of  $\text{SiS}$  in a  $Pm\bar{3}m$  structure (c) and  $\text{SiS}_3$  in an  $R3m$  structure (d).



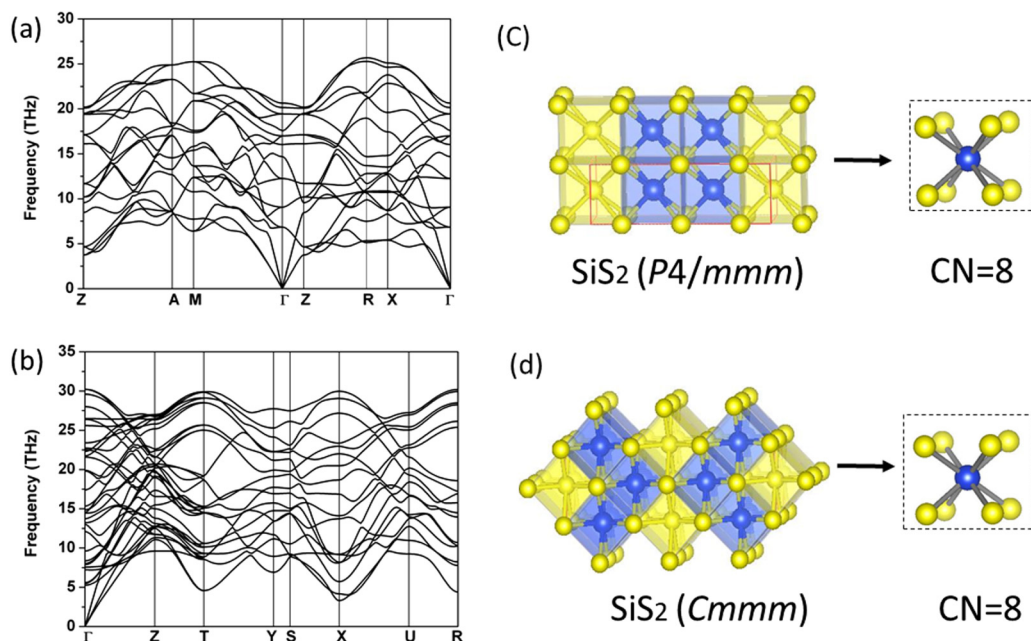


FIG. 4. Structures of the  $P4/mmm$  (a) and  $Cmmm$  (b) phases of  $\text{SiS}_2$ . The Si atoms are eightfold coordinated by S in both structure, forming  $\text{SiS}_8$  polyhedra. Phonon-dispersion curves for the  $P4/mmm$  phase of  $\text{SiS}_2$  at 300 GPa (c) and the  $Cmmm$  phase of  $\text{SiS}_2$  at 450 GPa (d).

We then took the HP eightfold-coordinated phases ( $P4/mmm$  and  $Cmmm$ ) of  $\text{SiS}_2$  as prototype structures for other IV–VI  $\text{AB}_2$  compounds and examined their stabilities. Unfortunately, we found that both these eightfold-coordinated phases are thermodynamically unstable comparing to the known four-, six-, nine-, and tenfold-coordinated phases of  $\text{AB}_2$ . Furthermore, we have explored the other possible  $\text{AB}_2$  structures with eightfold-coordinated A atoms at HP using CALYPSO. Our results demonstrated that four-, six-, nine-, and tenfold coordination are all favorable over eightfold coordination in all such  $\text{AB}_2$  compounds. In other words, none of the IV–VI  $\text{AB}_2$  compounds that we have considered form

an eightfold-coordinated structure as the stable HP phase (Fig. 5).

Our predicted  $Pm-3m$  phase for  $\text{SiS}$  may be among the first group IV–VI compounds to display eightfold coordination of the group-IV element. By replacing Si and S with heavier elements to consider the possibility of forming similar compounds in the IV–VI groups, the enthalpy difference of  $\text{AB}_2$  (e.g.,  $\text{GeSe}_2$ ,  $\text{SnSe}_2$ ) with respect to decomposition into stoichiometric  $\text{AB}$  and  $\text{AB}_3$  was calculated at pressures up to 150 GPa. Although the relative stabilities of their different compositions were not considered, the resulting enthalpy differences ( $2\text{GeSe}_2 \rightarrow \text{GeSe} + \text{GeSe}_3$ ) indicate that similar

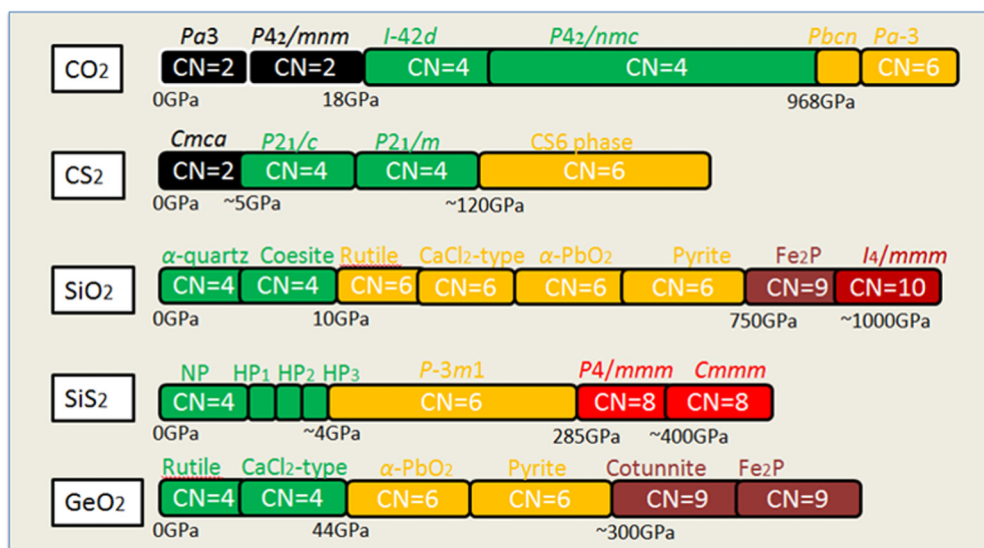


FIG. 5. Comparison of the stability ranges and the silicon coordination number of  $\text{SiS}_2$  under pressure with those in its isovalent IV–VI  $\text{AB}_2$  compounds, including  $\text{CO}_2$ ,  $\text{CS}_2$ ,  $\text{SiO}_2$ , and  $\text{GeO}_2$ .

eightfold-coordinated phase of GeSe may be formed at a lower critical pressure of  $\sim 120$  GPa. These results illustrate and highlight the fact that pressure can be deployed as a powerful tool in the search for novel materials and in the development of our understanding of the principles of chemical crystallography.

#### IV. CONCLUSIONS

In summary, we have systematically explored the phase stabilities and crystal structures of a range of materials with stoichiometries of  $\text{Si}_x\text{S}_{1-x}$  under HP using the CALYPSO method in combination with *ab initio* electronic band-structure framework. Our results reveal that  $\text{SiS}_2$  is the only stable stoichiometry below 155 GPa. Remarkably, this phase becomes unstable and decomposes into a mixture of stoichiometric phases  $\text{SiS}$  and  $\text{SiS}_3$  at higher pressure. The  $\text{SiS}$  phase adopts a high-symmetry  $Pm\bar{3}m$  structure consisting of a Si in eightfold-coordinated face-sharing  $\text{SiS}_8$

polyhedra, while  $\text{SiS}_3$  crystallizes an  $R3m$  structure consisting of ninefold-coordinated silicon in  $\text{SiS}_9$  polyhedra. In addition, the isovalent IV–VI  $AB_2$  compounds ( $\text{CO}_2$ ,  $\text{CS}_2$ ,  $\text{SiO}_2$ , and  $\text{GeO}_2$ ) are all found to avoid structures with eightfold-coordinated group-IV atoms. Our predicted  $\text{SiS}$  phase is identified as among the first group IV–VI compound containing eightfold-coordinated group-IV atoms, and our predicted  $\text{SiS}_3$  phase is a silicon sulfide material in which silicon is ninefold coordinated.

#### ACKNOWLEDGMENTS

We acknowledge funding from the National Natural Science Foundation of China (Grants No. 11604270 and No. 11704050), and the Fundamental Research Funds for the Central Universities (Grants No. 2682017CX052 and No. 2018GF08). S.A.T.R. is supported by NERC Grant No. NE/P012167/1. X.F. is grateful for China Scholarship Council.

Y.C. and X.F. contributed equally to this work.

- 
- [1] L. Stixrude, N. de Koker, N. Sun, M. Mookherjee, and B. B. Karki, *Earth Planet. Sci. Lett.* **278**, 226 (2009).
  - [2] W. B. Tonks and H. J. Melosh, *J. Geophys. Res. Planet* **98**, 5319 (1993).
  - [3] E. Herbst, T. J. Millar, S. Wlodek, and D. K. Bohme, *Astron. Astrophys.* **222**, 205 (1989).
  - [4] D. F. Dickinson and E. N. R. Kuiper, *Astrophys. J.* **247**, 112 (1981).
  - [5] M. Santoro and F. A. Gorelli, *Chem. Soc. Rev.* **35**, 918 (2006).
  - [6] C. S. Yoo, *Phys. Chem. Chem. Phys.* **15**, 7949 (2013).
  - [7] J. S. Tse, D. D. Klug, Y. Le Page, and M. Bernasconi, *Phys. Rev. B* **56**, 10878 (1997).
  - [8] M. T. Dove, M. S. Craig, D. A. Keen, W. G. Marshall, S. A. T. Redfern, K. O. Trachenko, and M. G. Tucker, *Mineral. Mag.* **64**, 569 (2000).
  - [9] J. Haines, J. M. Léger, C. Chateau, and A. S. Pereira, *Phys. Chem. Miner.* **27**, 575 (2000).
  - [10] Z. Łodziańska, K. Parlinski, and J. Hafner, *Phys. Rev. B* **63**, 134106 (2001).
  - [11] P. F. Yuan and Z. J. Ding, *J. Phys. Chem. Solids* **68**, 1841 (2007).
  - [12] R. P. Dias, C.-S. Yoo, V. V. Struzhkin, M. Kim, T. Muramatsu, T. Matsuoka, Y. Ohishi, and S. Sinogeikin, *Proc. Natl. Acad. Sci. USA* **110**, 11720 (2013).
  - [13] V. B. Prakapenka, L. S. Dubrovinsky, G. Shen, M. L. Rivers, S. R. Sutton, V. Dmitriev, H. P. Weber, and T. L. Bihan, *Phys. Rev. B* **67**, 132101 (2003).
  - [14] Y. Hu, B. Kiefer, C. R. Bina, D. Zhang, and P. K. Dera, *Geophys. Res. Lett.* **44**, 22 (2017).
  - [15] O. Tschauner, C. Ma, J. R. Beckett, C. Prescher, V. B. Prakapenka, and G. R. Rossman, *Science* **346**, 1100 (2014).
  - [16] T. Ishii, H. Kojitani, and M. Akaogi, *Earth. Planet. Sci. Lett.* **309**, 185 (2011).
  - [17] C. Prescher, V. B. Prakapenka, J. Stefanski, S. Jahn, L. B. Skinner, and Y. Wang, *Proc. Natl. Acad. Sci. USA* **114**, 10041 (2017).
  - [18] Y. Kono, C. Kenney-Benson, D. Ikuta, Y. Shibazaki, Y. Wang, and G. Shen, *Proc. Natl. Acad. Sci. USA* **113**, 3436 (2016).
  - [19] T. Tsuchiya and J. Tsuchiya, *Proc. Natl. Acad. Sci. USA* **108**, 1252 (2011).
  - [20] M. J. Lyle, C. J. Pickard, and R. J. Needs, *Proc. Natl. Acad. Sci. USA* **112**, 6898 (2015).
  - [21] H. Dekura, T. Tsuchiya, and J. Tsuchiya, *Phys. Rev. B* **83**, 134114 (2011).
  - [22] E. Zintl and K. Z. Loosen, *Phys. Chem. (Leipzig)* **174**, 301 (1935).
  - [23] T. A. Guseva, K. P. Burdina, and K. N. Semenenko, *Khimiya* **32**, 85 (1991).
  - [24] D. I. Bletskan, V. V. Vakulchak, and K. E. Glukhov, *Appl. Phys. A* **117**, 1499 (2014).
  - [25] J. Evers, P. Mayer, L. Möckl, G. Oehlinger, R. Köppe, and H. Schnöckel, *Inorg. Chem.* **54**, 1240 (2015).
  - [26] D. Plašienka, R. Martoňák, and E. Tosatti, *Sci. Rep.* **6**, 37694 (2016).
  - [27] Y. Wang, S.-Q. Jiang, A. F. Goncharov, F. A. Gorelli, X.-J. Chen, D. Plašienka, R. Martoňák, E. Tosatti, and M. Santoro, *J. Chem. Phys.* **148**, 014503 (2018).
  - [28] J. Evers, L. Möckl, G. Oehlinger, R. Köppe, H. Schnöckel, O. Barkalov, S. Medvedev, and P. Naumov, *Inorg. Chem.* **56**, 372 (2017).
  - [29] Y. Wang, J. Lv, L. Zhu, and Y. Ma, *Phys. Rev. B* **82**, 094116 (2010).
  - [30] Y. Wang, J. Lv, L. Zhu, and Y. Ma, *Comput. Phys. Commun.* **183**, 2063 (2012).
  - [31] J. Lv, Y. Wang, L. Zhu, and Y. Ma, *Phys. Rev. Lett.* **106**, 015503 (2011).
  - [32] L. Zhu, H. Liu, C. J. Pickard, G. Zou, and Y. Ma, *Nat. Chem.* **6**, 644 (2014).
  - [33] M. Hellenbrandt, *Crys. Rev.* **10**, 17 (2004).
  - [34] A. Jain, S. P. Ong, G. Hautier, W. Chen, W. D. Richards, S. Dacek, S. Cholia, D. Gunter, D. Skinner, G. Ceder, and K. A. Persson, *APL Mater.* **1**, 011002 (2013).
  - [35] G. Kresse and D. Joubert, *Phys. Rev. B* **59**, 1758 (1999).

- [36] J. P. Perdew, K. Burke, and M. Ernzerhof, [Phys. Rev. Lett. \*\*77\*\*, 3865 \(1996\)](#).
- [37] P. E. Blochl, [Phys. Rev. B \*\*50\*\*, 17953 \(1994\)](#).
- [38] H. J. Monkhorst and J. D. Pack, [Phys. Rev. B \*\*13\*\*, 5188 \(1976\)](#).
- [39] A. Togo and I. Tanaka, [Scr. Mater. \*\*108\*\*, 1 \(2015\)](#).
- [40] H. Katzke, U. Bismayer, and P. Tolédano, [Phys. Rev. B \*\*73\*\*, 134105 \(2006\)](#).
- [41] M. Monni, F. Bernardini, A. Sanna, G. Profeta, and S. Massidda, [Phys. Rev. B \*\*95\*\*, 064516 \(2017\)](#).
- [42] O. Degtyareva, E. Gregoryanz, M. Somayazulu, P. Dera, H.-k. Mao, and R. J. Hemley, [Nat. Mater. \*\*4\*\*, 152 \(2005\)](#).
- [43] C. Lu, M. Miao, and Y. Ma, [J. Am. Chem. Soc. \*\*135\*\*, 14167 \(2013\)](#).
- [44] V. Iota and C. S. Yoo, [Phys. Rev. Lett. \*\*86\*\*, 5922 \(2001\)](#).
- [45] R. Martoňák, D. Donadio, A. R. Oganov, and M. Parrinello, [Nat. Mater. \*\*5\*\*, 623 \(2006\)](#).
- [46] A. R. Oganov, M. J. Gillan, and G. D. Price, [Phys. Rev. B \*\*71\*\*, 064104 \(2005\)](#).